Perfect localization on flat-band binary one-dimensional photonic lattices

Gabriel Cáceres-Aravena and Rodrigo A. Vicencio

Departamento de Física and Millennium Institute for Research in Optics (MIRO), Facultad de Ciencias Físicas y Matemáticas,
Universidad de Chile, Santiago, Chile

We can generate the conditions for observing flat bands on initially trivial lattices by, for example, exciting a given system simultaneously with different orthogonal states. In this work, we demonstrate that a one-dimensional binary lattice supports always a trivial flat band, which is formed by isolated single-site vertical dipolar states. These flat-band modes correspond to the highest localized modes for any discrete system, without the need of any additional mechanism like, e.g., disorder or nonlinearity. By fulfilling a specific relation between lattice parameters, an extra flat band can be excited as well, with modes composed by fundamental and dipolar states that occupy only three lattice sites. Additionally, by inspecting the lattice edges, we are able to construct analytical Shockley surface modes, which can be compact or present staggered or unstaggered tails. We believe that our proposed model could be a good candidate for observing transport and localization phenomena on a simple one-dimensional linear photonic lattice.

I. INTRODUCTION

The propagation of waves in periodic systems are the natural framework to explore transport and localization phenomena in diverse fields of physics [1–3]. For example, the first experimental observation of Anderson-like localization in disordered linear systems [4] was made in 2007, in two-dimensional (2D) induced photonic lattices [5] and, subsequently, in fabricated one-dimensional (1D) waveguide arrays [6]. More recently, an important theoretical and experimental interest on flat-band (FB) systems has emerged [7–13], showing interesting localization and transport properties on linear lattices. The current experimental techniques allow direct and indirect excitation of flat-band phenomena [14–25], which is associated with destructive interference on specific lattice geometries. Specificaly, a Lieb photonic lattice was chosen to demonstrate, for the first time in any physical system, the existence of FB localized states [14,15]. A FB lattice geometry allows a precise cancellation of amplitudes outside the FB mode area, which effectively cancels the transport of energy across the system. Flat-band systems possess a linear spectrum where at least one band is completely flat or thin compared to the next energy gap. This implies the need to have a system with a unit cell composed of at least two sites and, therefore, at least two bands [8,26]. In this sense, the existence of flat bands in simple one-dimensional systems is generally thought to be physically impossible. However, quasi-1D systems (i.e., systems possessing a one-dimensional extension plus some ramifications away from the main axis) naturally present unit cells composed of more than one site, becoming good candidates for this kind of phenomenology [18–20,25,27]. In general, light propagating in FB lattices will experience zero or very low diffraction, when exciting some specific sites at the unit cell, as has been shown experimentally [18,28].

A very interesting feature of flat-band systems is the possibility to construct highly localized eigenmodes by means of a destructive linear combination of extended linear wave functions [7,29]. These FB states are spatially compact, occupy only few lattice sites, and rapidly decay to a completely zero tail as soon as a destructive interference condition is fulfilled [8]. This is a very remarkable property because FB lattices naturally generate localized structures in a linear regime, with a localization length of the order of a single unit cell. Moreover, as these linear localized modes posses all the same frequency, they are completely degenerate and any linear combination of them will also be a stable propagating solution. This can be used to achieve a nondiffractive transmission of optically codified information [14,16,17,20,21,29,30].

Almost all studies on photonic lattices have considered single-mode excitation only. This has been reinforced due to the experimental complexity in the excitation of higher-order modes on a given lattice system, which has found a partial solution only by the implementation of a selective *p*-band population in cold-atom systems [31,32] and micropillar arrays [33]. But, optical waveguides can also host higher order modes, depending on the specific experimental parameters used to perform the experiment (waveguide arrays are typically fabricated considering single-mode waveguides at a given wavelength; however, by reducing this parameter higher-order modes can be excited as well). Their excitation could promote richer dynamics and new interesting phenomena, as has been suggested for cold atoms loaded in optical potentials [34–37]. However, a precise excitation of dipolar states became possible very recently in optical waveguide lattices by using an image generator setup based on spatial light modulators [21,38]. There, a well-defined contrast between the transport of fundamental and dipolar states was shown clearly. The possibility to experimentally excite and control higher band excitations, in optical lattice systems, creates a venue in which the study of remarkable properties of correlated systems—such as superfluidity,

superconductivity, organic ferromagnetic, antiferromagnetic ordering, among others—could become a concrete possibility [34–37,39].

As is well known, diverse mechanisms have been proposed over several years to achieve stable energy localization on a lattice; for example, disorder [5,6], impurities and defects [40,41], and even nonlinearity [42–44]. However, all these mechanisms necessarily destroy the periodicity of the system, which finally has important consequences on the transport of energy across the lattice. In the present work, we propose a model for the observation of FB properties. We focus on a binary 1D lattice, which to our knowledge corresponds to the simplest physical configuration for studying FB localization. We specifically concentrate on proposing a simple—completely periodic—system which could show the conditions to observe localization and transport of energy on a linear regime. By exciting a system with different orthogonal states we effectively increase the dimension of the system from 1D to quasi-1D, allowing a subsequent increment of the unit cell. Our model possesses a trivial FB which corresponds to an effectively isolated dipolar mode. This mode is localized at a single waveguide corresponding, therefore, to the most localized FB state. By precisely tuning the model parameters, we observe that a second FB can be excited as well, with states occupying only three lattice sites. In addition, we explore edge localization and find analytical Shockley edge modes with different decaying properties. At the end, we find an additional flat band when assuming equal propagation constants on both orthogonal states.

II. MODEL

We study the propagation of light, in weakly coupled waveguide arrays, based on a coupled mode approach which originates from a paraxial wave equation and ends up with a set of discrete linear Schrödinger-like equations [1,2]. This approach assumes an evanescent interaction between the modes of neighboring waveguides, with a coupling coefficient defined via the superposition integral between both mode wave functions. Obviously, this interaction is negligible when waveguides are far away in distance and becomes physically relevant only when waveguides are close enough. Typical experiments on laser-written photonic lattices [45] define a distance of around 20 microns to correctly describe the system, assuming nearest-neighbor interactions only. In this work, we model a binary one-dimensional photonic lattice composed of an alternating configuration of waveguides, as shown in Fig. 1(a). (Different realizations of binary lattices have been studied in the context of photonic systems; for example, binary lattices with alternating propagation constants [46,47], alternating coupling coefficients [48], or simultaneously both [49].) We assume elliptically oriented waveguides, which are the standard geometry in laser-written systems [45], with the propagation coordinate z (dynamical variable) running perpendicular to the transversal waveguide profile. Additionally, we consider that each waveguide supports only two orthogonal modes, the fundamental (s) and the dipolar (p) ones. In general, a single waveguide possesses always at least one bound state, which corresponds to the symmetric s mode [50,51]. However, depending on the experimental
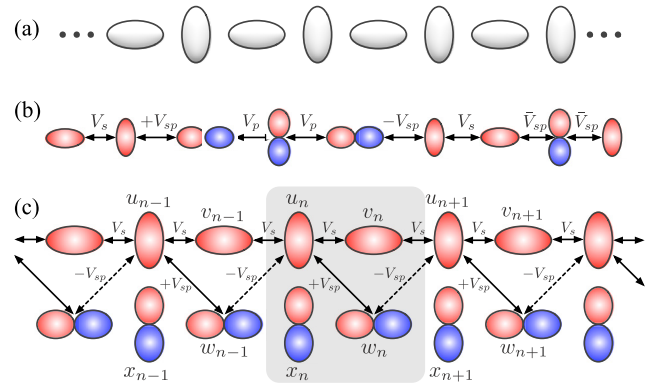

FIG. 1. (a) 1D-binary waveguide array. (b) Coupling interactions for this model (red represents a positive amplitude while blue a negative one). (c) Effective ribbon lattice when considering two modes per waveguide (the shaded area indicates the unit cell).

conditions, it is possible to directly excite higher-order states as, e.g., p modes [21,38]. For a given waveguide, having a defined geometry and refractive index contrast, the excitation wavelength can be tuned experimentally to excite higher-order states. As different modes have a different spatial configuration, there will be a natural mismatch in their propagation constants. This implies that $\beta_s \neq \beta_p$ [21], where β_i is the longitudinal propagation constant of the i mode at any lattice waveguide.

The possible interactions between modes at different neighboring waveguides are depicted in Fig. 1(b). Considering the symmetry of s and p wave functions, we construct a general evanescent interaction rule for our binary system: the coupling between s modes (defined as V_s) is always positive [52]; the coupling between p modes (V_p) as well as the coupling between s and vertical p modes ($\bar{V}_{sp}$) are always zero; the coupling between vertical s and horizontal p modes (V_{sp}) is defined positive when the s mode is at the left-hand side, if not a minus sign is applied. In general, due to the larger area occupied by p modes, $V_{sp} > V_s$. Having this in mind, we construct an effective ribbon lattice in Fig. 1(c) and write the effective dynamical equations as follows:

$$-i\frac{\partial u_n(z)}{\partial z} = \beta_s u_n + V_s(v_n + v_{n-1}) + V_{sp}(w_n - w_{n-1}),$$

$$-i\frac{\partial v_n(z)}{\partial z} = \beta_s v_n + V_s(u_{n+1} + u_n),$$

$$-i\frac{\partial x_n(z)}{\partial z} = \beta_p x_n,$$

$$-i\frac{\partial w_n(z)}{\partial z} = \beta_p w_n - V_{sp}(u_{n+1} - u_n). \tag{1}$$

Here, u_n and v_n (x_n and w_n) describe the amplitude of fundamental (dipolar) modes at the nth unit cell. The alternating orientation of our 1D binary lattice and the possibility of exciting two modes per waveguide generate a four-state effective system, which is described by these four coupled equations. It is important to mention that, in order to have an effective dynamical interaction between the s and the p modes, $\Delta\beta \equiv \beta_s - \beta_p$ has to be of the order of V_{sp}. If not, this detuning effectively decouples the interaction between these two modes

and they simply do not interact [21]. $\Delta\beta > 0$ for any optical media where the propagation constants of fundamental modes are always larger than the ones for excited states [1,21,38].

III. LINEAR SPECTRUM

We solve the linear spectrum of the system by inserting into (1) a standard plane-wave ansatz [8], of the form

$$\{u_n, v_n, x_n, w_n\}(z) = \{A, B, C, D\}\, e^{ikn} e^{i(\beta + \beta_p)z}.$$

With this, we assume that the wave propagation occurs along the horizontal direction only, k being equal to the normalized transversal wavevector. β represents the longitudinal propagation constant of the lattice eigenmodes (also known as supermodes), while β_i represents the longitudinal propagation constant of mode i on a single waveguide. Without loss of generality, we include a gauge transformation on β_p, with the purpose of reducing the model parameters and simplify the overall description. By doing this, we get a set of four coupled equations which can be written as follows:

$$\beta\Psi = \begin{pmatrix} \Delta\beta & V_s(1 + e^{-ik}) & 0 & V_{sp}(1 - e^{-ik}) \\ V_s(1 + e^{ik}) & \Delta\beta & 0 & 0 \\ 0 & 0 & 0 & 0 \\ V_{sp}(1 - e^{ik}) & 0 & 0 & 0 \end{pmatrix}\Psi,$$

(2)

with $\Psi \equiv \{A, B, C, D\}$. By solving this eigenvalue problem, we obtain four solutions, with three of them being determined by the following third-order equation:

$$\left[\beta(\Delta\beta - \beta)^2 - 4V_s^2\beta\cos^2\bar{k} + 4V_{sp}^2(\Delta\beta - \beta)\sin^2\bar{k}\right] = 0,$$

where $\bar{k} \equiv k/2$. These three bands are analytically nontrivial and have no simple and compact form for arbitrary parameters. Therefore, we show them graphically only in Figs. 2(a)–2(d), in the first Brillouin zone, using full black and orange lines. We also show in these figures (using dashed black lines) a completely constant solution

$$\beta_2 = 0,$$

which corresponds to the lattice second band, as defined below. This trivial and completely flat band is related to the excitation of isolated vertical p modes only. As these modes possess no coupling at all with nearest-neighbor waveguides, once they are excited they remain localized at the input position as long as the system length. This can be understood easily by directly integrating the third equation in (1), getting $x_n(z) = x_n(0) \exp\{i\beta_p z\}$; this is, therefore, a trivial stationary solution. In Fig. 2(e) we show a sketch of this FB state. This corresponds to the most localized FB state, which occupies only one site of the lattice. As this mode can be excited in every vertically oriented waveguide (using arbitrary amplitudes), this trivial band can be used, for example, to transmit optically codified information through this 1D lattice.

We observe that the linear spectrum is quite symmetric; therefore, we analyze the four linear bands considering an increasing order denoted by β_1, β_2, β_3, and β_4, as indicated in Fig. 2(a). At $k_x = 0$, band edges become
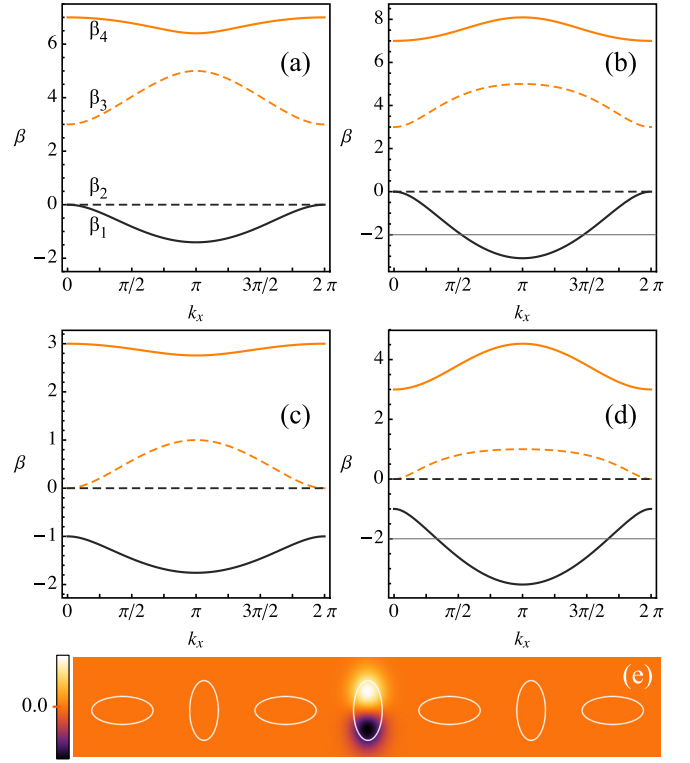
$$\{0, 0, \Delta\beta - 2V_s, \Delta\beta + 2V_s\}$$

FIG. 2. Linear spectrum for the 1D binary lattice. (a) $V_{sp} = 1.5$ and (b) 2.5, for $\Delta\beta = 5$. (c) $V_{sp} = 1.1$ and (d) 2.0, for $\Delta\beta = 1$. Full black, dashed black, dashed orange, and full orange correspond to β_1, β_2, β_3, and β_4 bands. (e) FB mode amplitude profile at $\beta_2 = 0$. In all the figures, we set $V_s = 1$.

for $\Delta\beta \geqslant 2V_s$, and

$$\{\Delta\beta - 2V_s, 0, 0, \Delta\beta + 2V_s\}$$

for $\Delta\beta < 2V_s$. At $k_x = \pi$, band edges are always

$$\left\{\frac{\Delta\beta - \sqrt{\Delta\beta^2 + 16V_{sp}^2}}{2}, 0, \Delta\beta, \frac{\Delta\beta + \sqrt{\Delta\beta^2 + 16V_{sp}^2}}{2}\right\},$$

as shown for some specific parameters in Figs. 2(a)–2(d). First of all, we notice that there is no gap between bands β_1, β_2, and β_3 for $\Delta\beta = 2V_s$. Then, there is a gap of size $\Delta\beta - 2V_s$, between bands β_2 and β_3 for $\Delta\beta \geqslant 2V_s$, and between bands β_1 and β_2 for $\Delta\beta < 2V_s$, which does not depend on the interaction between s and p modes. In contrast, the gap between bands β_3 and β_4 changes depending on the curvature of band β_4, which strongly depends on coupling V_{sp} as shown in Fig. 2. This change in the curvature necessarily implies that β_4 must be flat at some specific value of V_{sp}. By demanding that $\beta_4(0) = \beta_4(\pi)$, we obtain the following FB condition:

$$V_{sp}^{FB} \equiv V_s\sqrt{1 + \frac{\Delta\beta}{2V_s}}.$$

This mathematical relation is physical and experimentally possible due to the fact that $V_{sp} > V_s$, as expected considering the s and p mode profiles. If we fix coupling V_s, V_{sp}^{FB} grows monotonically as a function of detuning $\Delta\beta$. Once this condition is fulfilled, the fourth band becomes completely flat with
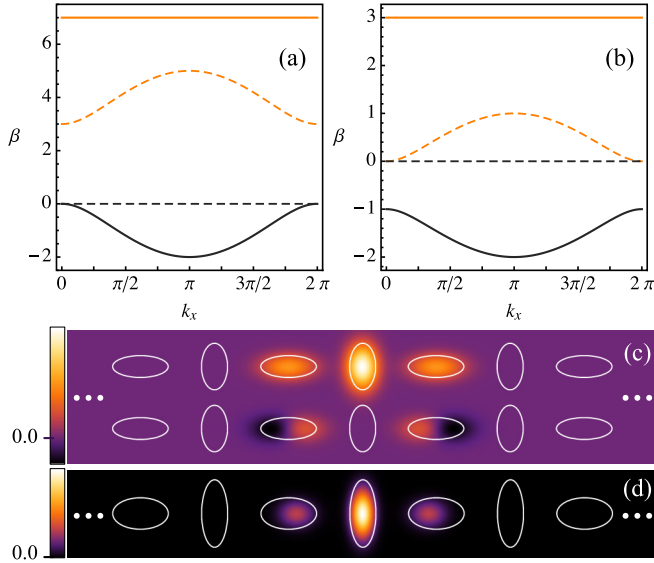
FIG. 3. Linear spectrum for (a) $\{\Delta\beta, V_{sp}^{FB}\} = \{5, 1.87\}$ and (b) $\{\Delta\beta, V_{sp}^{FB}\} = \{1, 1.22\}$. Full black, dashed black, dashed orange, and full orange correspond to β_1, β_2, β_3, and β_4 bands, respectively. (c) Effective amplitude and (d) intensity FB (β_4) mode profiles for $\Delta\beta = 1$. In all the figures, we set $V_s = 1$.

a value

$$\beta_4 = \Delta\beta + 2V_s,$$

as shown in Figs. 3(a) and 3(b) by a straight horizontal full orange line. We look for the eigenmode profile at this FB condition. We assume a center site n_0 and an arbitrary amplitude A, obtaining that

$$u_n = A\delta_{n,n_0}, \quad v_n = \left(\frac{A}{2}\right)(\delta_{n,n_0} + \delta_{n,n_0-1}),$$

$$x_n = 0, \quad w_n = \left(\frac{V_s A}{2V_{sp}^{FB}}\right)(\delta_{n,n_0} - \delta_{n,n_0-1}).$$

This profile is composed of both s and p modes simultaneously, and a sketch of it, on an effective ribbon lattice, is presented in Fig. 3(c). We observe that the dipolar mode is smaller in amplitude with a factor ~ 0.4, for the parameters used in this figure. As coupling V_{sp}^{FB} is larger than V_s, the mode amplitudes are compensated in order to satisfy a FB localization condition, which relies on destructive interference at specific connector sites [8]. Superposed s and p mode amplitudes give the FB mode intensity profile sketched in Fig. 3(d), for the 1D binary lattice system. The amplitudes beside the center show a shifted intensity with respect to the center of the waveguide, as expected from the superposition of fundamental and dipolar profiles at those sites. As a consequence, this localized state is very localized in space and perfectly compact.

A study of the transport in this lattice, performed by exciting a single vertical bulk site only (a deltalike input condition) would show a transition between dispersion (transport), localization (insulation), and transport again, while varying parameter V_{sp}. Localization would occur close to the FB condition V_{sp}^{FB}, while transport would manifest away this value.

This behavior is quite similar to the one found for sawtooth lattices [18], where a FB is formed only for a very specific condition between coupling constants. Therefore, our simple 1D binary model could show an insulator transition when coupling interaction V_{sp}/V_s is varied along the experiment. This could be demonstrated by fabricating several lattices having different refractive index profiles or directly shown by varying the temperature of a single binary lattice to achieve a tuning on propagation constants [53].

IV. EDGE STATES

When solving the eigenvalue problem (2), we look for solutions assuming an infinite lattice. Therefore, finite size effects, as for example linear edge modes, will not appear explicitly [18]. However, by numerically diagonalizing a finite lattice system, we find that an edge with a vertically oriented waveguide generates an exponentially decaying eigenmode, while a horizontal edge waveguide does not. In order to investigate this edge state, we consider a vertical waveguide at site $n = 1$ and assume the following ansatz [1,2,18]:

$$\{u_n, v_n, x_n, w_n\}(z) = \{A, B, C, D\}\epsilon^{n-1}e^{i\beta_e z}$$

for $n \geqslant 1$, with $|\epsilon| < 1$ (which implies an exponentially decaying state). A, B, and D correspond to the amplitudes of this mode to be determined by solving a set of coupled equations. We assume a zero amplitude for mode x_n ($C = 0$), due to the noninteraction of this mode with the rest of the system. (By taking $x_n \neq 0$ the frequency of this amplitude will be just zero, which does not necessarily coincides with the frequency of the edge mode β_e. Additionally, there is always a perfectly localized edge state $x_n = C\delta_{n,1}$, as a trivial FB solution.) We insert this ansatz into model (1) and write the equations for sites $n = 1$ and $n = 2$. We obtain two sets of three coupled equations, where the second set is recursively repeated for $n > 2$, which validates the proposed ansatz. These equations are the following:

$$\beta_e A = \beta_s A + V_s B + V_{sp} D,$$
$$\beta_e B = \beta_s B + V_s A(1 + \epsilon), \quad (3)$$
$$\beta_e D = \beta_p D + V_{sp} A(1 - \epsilon)$$

and

$$\beta_e A\epsilon = \beta_s A\epsilon + V_s B(1 + \epsilon) + V_{sp} D(\epsilon - 1),$$
$$\beta_e B\epsilon = \beta_s B\epsilon + V_s A\epsilon(1 + \epsilon), \quad (4)$$
$$\beta_e D\epsilon = \beta_p D\epsilon + V_{sp} A\epsilon(1 - \epsilon).$$

By applying some algebra to Eqs. (3) and (4), we obtain that

$$\left(\frac{D}{A}\right) = \left(\frac{V_s}{V_{sp}}\right)\gamma, \quad \epsilon = 2\gamma^2 - 1, \quad \beta_e = \beta_s + 2V_s\gamma,$$

with

$$\gamma \equiv \left(\frac{B}{A}\right) = \frac{\sqrt{\Delta\beta^2 V_s^2 + 16V_{sp}^2(V_s^2 + V_{sp}^2)} - \Delta\beta V_s}{4(V_s^2 + V_{sp}^2)}.$$

This expression satisfies that $0 < \gamma < 1$, which implies that $-1 < \epsilon < 1$; i.e., this edge state is exponentially localized at the surface when this surface has a vertically
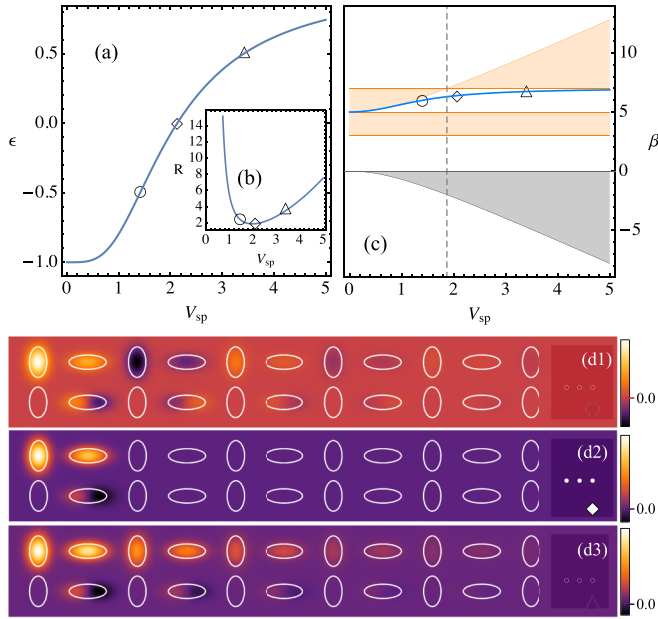
FIG. 4. (a) Decaying factor ϵ, (b) participation ratio R, and (c) propagation constant β_e versus coupling V_{sp}, for the edge mode (full blue line). Bands are plotted in (c) as shaded regions. (d1)–(d3) Effective edge mode amplitude profiles for V_{sp}: $\sqrt{2}$, $V_{sp}^{ce} = 2.13$, 3.43, respectively, labeled by a circle, a diamond, and a triangle in (a)–(d). $\Delta\beta = 5$ and $V_s = 1$.

oriented first waveguide. Additionally, as $V_{sp} > V_s$ then $(D/A) < (B/A)$; therefore, the edge localization is reinforced with a decreasing profile into the bulk of the system. In order to study the effective spatial size of these edge states, we compute an effective participation ratio, defined as $R \equiv [\sum_n(|u_n|^2 + |v_n|^2 + |x_n|^2 + |w_n|^2)]^2 / \sum_n(|u_n|^4 + |v_n|^4 + |x_n|^4 + |w_n|^4)$, obtaining

$$R = \frac{[1 + \gamma^2 + (V_s/V_{sp})^2\gamma^2]^2(1 + \epsilon^2)}{[1 + \gamma^4 + (V_s/V_{sp})^4\gamma^4] \quad (1 - \epsilon^2)}.$$

In order to characterize these states, we plot the decaying factor ϵ, the participation ratio R, and the frequency β_e versus the coupling V_{sp} in Figs. 4(a)–4(c), respectively, for some specific values of $\Delta\beta$ and V_s (the same phenomenology persists for different values). First of all, we observe that when coupling $V_{sp} \to 0$, B and D go to zero as well and the edge state bifurcates at the band center of a standard 1D lattice [1,2], with $\epsilon \to -1$, $R \to \infty$, and $\beta_e \to \beta_s$. This state coincides with the $\pi/2$ linear mode of a standard 1D lattice and has an effective spatial profile of only s-mode amplitudes. Once we increase the coupling V_{sp}, we observe that the decaying factor ϵ decreases in magnitude, being for example -0.5 for $V_{sp} \approx \sqrt{2}$. In this case, the edge mode has a staggered profile every two sites, as shown in Fig. 4(d1). After this, we obtain a perfectly localized edge state with an exactly zero tail ($\epsilon = 0$), as Fig. 4(d2) shows. This compact edge mode is obtained for the condition

$$V_{sp}^{ce} \equiv V_s\sqrt{1 + \frac{\Delta\beta}{\sqrt{2}V_s}} > V_{sp}^{FB}.$$

This state is similar to the edge mode found in sawtooth lattices [18], when different amplitudes destructively interfere at the connector sites of the lattice, in this case at the second vertically oriented waveguide. Although this profile corresponds to a perfectly compact edge state, which occupies only two sites of the lattice, with a mixed s-p profile, it is not the most localized edge state in this 1D binary system. In fact, for the parameters considered in Fig. 4, the perfectly compact edge state at $V_{sp}^{ce} = 2.13$ has a participation ratio of $R = 1.92$, while the minimum participation ratio $R = 1.89$ occurs for $V_{sp} = 1.98$.

After this regime, the decaying factor starts to grow slowly and profiles become completely unstaggered in their phase structure, as in the example shown in Fig. 4(d3) for $\epsilon \approx 0.5$. By a further increment of V_{sp}, ϵ slowly tends to its upper bound 1, implying a smooth increment of R. The propagation constant β_e slowly tends to $\Delta\beta + 2V_s$, which coincides with the bottom of band β_4. It is important to notice that the FB condition at $V_{sp}^{FB} = 1.87$ [see dashed vertical line in Fig. 4(c)] produces an exchange on band β_4, in which the fundamental unstaggered mode passes from being at the top of the band for $V_{sp} = 0$ to being at the band bottom for $V_{sp} > V_{sp}^{FB}$, as shown in Fig. 4(c). Finally, a larger V_{sp} coefficient implies that $\delta \to 1$, with $B/A \to 1$ and $D/A \to 0$. Therefore, the lattice effectively transforms into a standard 1D system, with a homogenous spatial profile of s-mode amplitudes only, which coincides with a standard unstaggered fundamental mode. Here, although V_{sp} is large compared to V_s, there is a consecutive cancellation of dipolar amplitudes D, due to the alternated sign of this coupling interaction.

Both limits ($V_{sp} \to 0, \infty$) gives us an extended mode which coincides with the β_4-band modes of standard 1D lattices, where no surface states exist without distorting the lattice border [54–56]. As we observe in Fig. 4(c), β_e is only allowed to exist in the region $\{\Delta\beta, \Delta\beta + 2V_s\}$, and edge modes behave quite similarly to the one found in a sawtooth lattice [18], including the band twist at the FB critical parameter. In that case, authors associated the edge modes to Shockley-like surface states [57], but they also mentioned that these states existed due to a reduction of nearest neighbors at the right surface, which generates an effective defect [28]. We have checked the extended linear modes of our model for different edge terminations. We have found that, in the presence of vertically oriented surface waveguides (in one or both edges), there is always a nonsymmetric termination of extended states, which appears typically in lattices presenting edge defects [47,49]. Typical extended modes of standard lattices have a node at the edges and they are symmetric with respect to the lattice system. That means that there is an effective distortion of the lattice at the right border, which naturally produces Tamm-like edge states [58]. When considering horizontally oriented waveguides at the border, we immediately get a node at the right edge, similar to a standard 1D lattice picture, which has no surface states at all [54–56].

V. $\Delta\beta = 0$ LIMIT

Although the case $\Delta\beta = 0$ corresponds to a nonphysical solution in our photonic system [21,50,51], it becomes
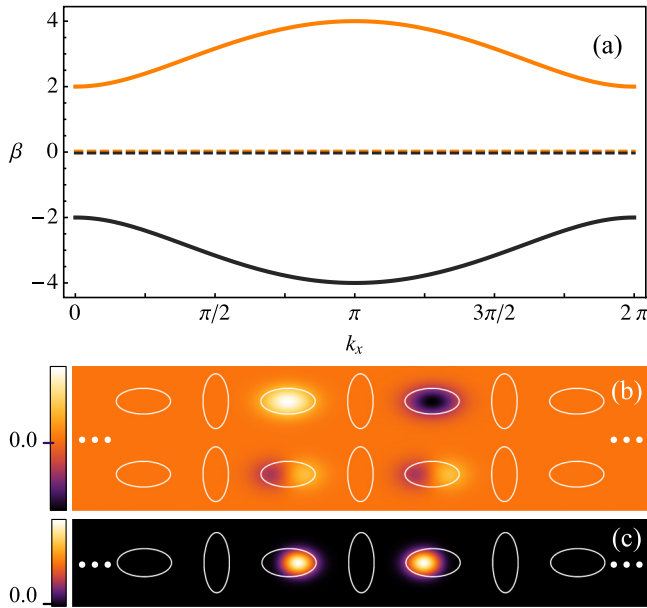
FIG. 5. (a) Linear spectrum for $\Delta\beta = 0$, $V_s = 1$, and $V_{sp} = 2.0$. Full black, dashed black, dashed orange, and full orange correspond to β_1, β_2, β_3, and β_4 bands, respectively. (b) Effective amplitude and (c) intensity FB (β_3) mode profiles.

interesting to analyze it due to its phenomenology. By applying this condition, the eigenvalue problem (2) gives four simple solutions:

$$\beta = 0, 0, \pm 2\sqrt{V_s^2 \cos^2 \bar{k} + V_{sp}^2 \sin^2 \bar{k}}.$$

We plot the linear spectrum in Fig. 5(a) and observe two opposite dispersive bands, showing a particle-hole symmetry [59] in which for any value of k_x there are two eigenfrequencies $\pm\beta(k)$. Additionally, we found two flat bands at exactly the same frequency $\beta_2 = \beta_3 = 0$. The first one is the previously found trivial FB $\beta_2 = 0$, which consists on single-site vertical dipolar states. The second FB is generated by a combination of horizontal s and p modes, whose mode profiles consist of four amplitudes different from zero, having the following structure:

$$u_n = 0, \quad v_n = A(\delta_{n,n_0} - \delta_{n,n_0+1}),$$

$$x_n = 0, \quad w_n = -\left(\frac{V_s}{V_{sp}}\right)A(\delta_{n,n_0} + \delta_{n,n_0+1}).$$

This amplitude profile is sketched in Fig. 5(b), with the corresponding intensity profile shown in Fig. 5(c). We observe how a perfect cancellation of amplitudes, at connector sites,

allows the formation of a highly localized pattern, which has only two sites different from zero. In terms of localization area, this state is comparable with the one found for diamond lattices [19], which is the most localized FB state observed experimentally up to now.

VI. CONCLUSIONS

In conclusion, we have proposed a model for the study of localization and transport of light in photonic lattices. In particular, our model consists of a rather simple 1D lattice having alternating orientation of elliptical waveguides. We found that, by assuming two modes, s and p, per site, a quasi-1D effective ribbon system emerges, which describes the light dynamics on this lattice. We found that there is always a FB on this system, which corresponds to vertically isolated dipolar states. These FB modes occupy a single site only, and are therefore the most localized FB states of any lattice configuration. By fulfilling a specific relation between lattice parameters, we found that a second nontrivial FB appears, which is composed of a hybridized state with s and p modes excited simultaneously. These FB states occupy only three lattice sites, with a rapidly decaying and perfectly compact profile. By investigating the edges of this lattice, we found that Shockley-like surface states exist on the system for edges having vertically oriented waveguides. We obtained an analytical expression for them and found that they could show different properties depending on the lattice parameters. At the end, we explored the case $\Delta\beta = 0$ and found two dispersive and two flat bands for this binary 1D system.

We believe that our simple model could show interesting features for nondiffractive image transmission applications as well as for presenting different transport properties depending on the input condition. For example, by exciting a vertically oriented waveguide with a fundamental state we would simply observe transport, while using a dipolar excitation would produce perfect localization, without the need to apply any extra interaction. This could be useful to excite two completely different states on the system, which could be of interest for optical signal processing.

[1] F. Lederer, G. I. Stegeman, D. N. Christodoulides, G. Assanto, M. Segev, and Y. Silberberg, Phys. Rep. **463**, 1 (2008).

[2] S. Flach and A. V. Gorbach, Phys. Rep. **467**, 1 (2008).

[3] D. K. Campbell, S. Flach, and Yu. S. Kivshar, Phys. Today **57**(1), 43 (2004).

[4] P. W. Anderson, Phys. Rev. **109**, 1492 (1958).

[5] T. Schwartz, G. Bartal, S. Fishman, and M. Segev, Nature (London) **446**, 52 (2007).

[6] Y. Lahini, A. Avidan, F. Pozzi, M. Sorel, R. Morandotti, D. N. Christodoulides, and Y. Silberberg, Phys. Rev. Lett. **100**, 013906 (2008).

[7] D. L. Bergman, C. Wu, and L. Balents, Phys. Rev. B **78**, 125104 (2008).

[8] L. Morales-Inostroza and R. A. Vicencio, Phys. Rev. A **94**, 043831 (2016).

[9] D. Leykam, A. Andreanov, and S. Flach, Adv. Phys. X **3**, 1473052 (2018).

[10] D. Leykam and S. Flach, APL Photonics **3**, 070901 (2018).

[11] B. Pal and K. Saha, Phys. Rev. B **97**, 195101 (2018).

[12] J.-W. Rhim and B.-J. Yang, Phys. Rev. B **99**, 045107 (2019).

[13] N. Myoung, H. C. Park, A. Ramachandran, E. Lidorikis, and J.-W. Ryu, Sci. Rep. **9**, 2862 (2019).

[14] R. A. Vicencio, C. Cantillano, L. Morales-Inostroza, B. Real, C. Mejía-Cortés, S. Weimann, A. Szameit, and M. I. Molina, Phys. Rev. Lett. **114**, 245503 (2015).

[15] S. Mukherjee, A. Spracklen, D. Choudhury, N. Goldman, P. Öhberg, E. Andersson, and R. R. Thomson, Phys. Rev. Lett. **114**, 245504 (2015).

[16] Y. Zong, S. Xia, L. Tang, D. Song, Y. Hu, Y. Pei, J. Su, Y. Li, and Z. Chen, Opt. Express **24**, 8877 (2016).

[17] S. Xia, Y. Hu, D. Song, Y. Zong, L. Tang, and Z. Chen, Opt. Lett. **41**, 1435 (2016).

[18] S. Weimann, L. Morales-Inostroza, B. Real, C. Cantillano, A. Szameit, and R. A. Vicencio, Opt. Lett. **41**, 2414 (2016).

[19] S. Mukherjee and R. R. Thomson, Opt. Lett. **40**, 5443 (2015).

[20] B. Real, C. Cantillano, D. López-González, A. Szameit, M. Aono, M. Naruse, S. Kim, K. Wang, and R. A. Vicencio, Sci. Rep. **7**, 15085 (2017).

[21] C. Cantillano, S. Mukherjee, L. Morales-Inostroza, B. Real, G. Cáceres-Aravena, C. Hermann-Avigliano, R. R. Thomson, and R. A. Vicencio, New J. Phys. **20**, 033028 (2018).

[22] Z. Lin, J.-H. Choi, Q. Zhang, W. Qin, S. Yi, P. Wang, L. Li, Y. Wang, H. Zhang, Z. Sun, L. Wei, S. Zhang, T. Guo, Q. Lu, J.-H. Cho, C. Zeng, and Z. Zhang, Phys. Rev. Lett. **121**, 096401 (2018).

[23] G.-B. Jo, J. Guzman, C. K. Thomas, P. Hosur, A. Vishwanath, and D. M. Stamper-Kurn, Phys. Rev. Lett. **108**, 045305 (2012).

[24] F. Baboux, L. Ge, T. Jacqmin, M. Biondi, E. Galopin, A. Lemaître, L. Le Gratiet, I. Sagnes, S. Schmidt, H. E. Türeci, A. Amo, and J. Bloch, Phys. Rev. Lett. **116**, 066402 (2016).

[25] Y.-X. Xiao, G. Ma, Z.-Q. Zhang, and C. T. Chan, Phys. Rev. Lett. **118**, 166803 (2017).

[26] B. Pal, Phys. Rev. B **98**, 245116 (2018).

[27] S. Flach, D. Leykam, J. D. Bodyfelt, P. Matthies, and A. S. Desyatnikov, Europhys. Lett. **105**, 30001 (2014).

[28] D. Guzmán-Silva, C. Mejía-Cortés, M. A. Bandres, M. C. Rechtsman, S. Weimann, S. Nolte, M. Segev, A. Szameit, and R. A. Vicencio, New J. Phys. **16**, 063061 (2014).

[29] S. Xia, A. Ramachandran, S. Xia, D. Li, X. Liu, L. Tang, Y. Hu, D. Song, J. Xu, D. Leykam, S. Flach, and Z. Chen, Phys. Rev. Lett. **121**, 263902 (2018).

[30] R. A. Vicencio and C. Mejía-Cortés, J. Opt. **16**, 015706 (2014).

[31] G. Wirth, M. Ölschläger, and A. Hemmerich, Nat. Phys. **7**, 147 (2011).

[32] S. Klembt, T. H. Harder, O. A. Egorov, K. Winkler, H. Suchomel, J. Beierlein, M. Emmerling, C. Schneider, and S. Höfling, Appl. Phys. Lett. **111**, 231102 (2017).

[33] M. Milićević, T. Ozawa, G. Montambaux, I. Carusotto, E. Galopin, A. Lemaître, L. Le Gratiet, I. Sagnes, J. Bloch, and A. Amo, Phys. Rev. Lett. **118**, 107403 (2017).

[34] C. Wu, D. Bergman, L. Balents, and S. Das Sarma, Phys. Rev. Lett. **99**, 070401 (2007).

[35] X. Li, E. Zhao, and W. V. Liu, Nat. Commun. **4**, 1523 (2013).

[36] S. Yin, J. E. Baarsma, M. O. J. Heikkinen, J.-P. Martikainen, and P. Törmä, Phys. Rev. A **92**, 053616 (2015).

[37] X. Li and W. V. Liu, Rep. Prog. Phys. **79**, 116401 (2016).

[38] C. Cantillano, L. Morales-Inostroza, B. Real, S. Rojas-Rojas, A. Delgado, A. Szameit, and R. A. Vicencio, Sci. Bull. **62**, 339 (2017).

[39] M. Hatanaka, Theor. Chem. Acc. **129**, 151 (2011).

[40] F. Fedele, J. Yang, and Z. Chen, Opt. Lett. **30**, 1506 (2005).

[41] I. Makasyuk, Z. Chen, and J. Yang, Phys. Rev. Lett. **96**, 223903 (2006).

[42] H. S. Eisenberg, Y. Silberberg, R. Morandotti, A. R. Boyd, and J. S. Aitchison, Phys. Rev. Lett. **81**, 3383 (1998).

[43] J. W. Fleischer, T. Carmon, M. Segev, N. K. Efremidis, and D. N. Christodoulides, Phys. Rev. Lett. **90**, 023902 (2003).

[44] A. Szameit, D. Blömer, J. Burghoff, T. Schreiber, T. Pertsch, S. Nolte, A. Tünnermann, and F. Lederer, Opt. Express **13**, 10552 (2005).

[45] A. Szameit, D. Blömer, and J. Burghoff, Appl. Phys. B **82**, 507 (2006).

[46] A. A. Sukhorukov and Y. S. Kivshar, Opt. Lett. **27**, 2112 (2002).

[47] N. Malkova, I. Hromada, X. Wang, G. Bryant, and Z. Chen, Opt. Lett. **34**, 1633 (2009).

[48] R. A. Vicencio and M. Johansson, Phys. Rev. A **79**, 065801 (2009).

[49] N. Malkova, I. Hromada, X. Wang, G. Bryant, and Z. Chen, Phys. Rev. A **80**, 043806 (2009).

[50] A. W. Snyder and W. R. Young, J. Opt. Soc. Am. **68**, 297 (1978).

[51] D. Gloge, Appl. Opt. **10**, 2252 (1971).

[52] For purely evanescent coupling, V_s is always larger than zero. However, there are some physical waveguide configurations where this could present a different form [60].

[53] T. Pertsch, P. Dannberg, W. Elflein, A. Bräuer, and F. Lederer, Phys. Rev. Lett. **83**, 4752 (1999).

[54] M. I. Molina, R. A. Vicencio, Yu. S. Kivshar, Opt. Lett. **31**, 1693 (2006).

[55] C. R. Rosberg, D. N. Neshev, W. Krolikowski, A. Mitchell, R. A. Vicencio, M. I. Molina, and Yu. S. Kivshar, Phys. Rev. Lett. **97**, 083901 (2006).

[56] E. Smirnov, M. Stepić, C. E. Rüter, D. Kip, and V. Shandarov, Opt. Lett. **31**, 2338 (2006).

[57] W. Shockley, Phys. Rev. **56**, 317 (1939).

[58] I. Tamm, Z. Phys. **76**, 849 (1932).

[59] J. He, Y.-X. Zhu, Y.-J. Wu, L.-F. Liu, Y. Liang, and S.-P. Kou, Phys. Rev. B **87**, 075126 (2013).

[60] N. K. Efremidis, P. Zhang, Z. Chen, D. N. Christodoulides, C. E. Rüter, and D. Kip, Phys. Rev. A **81**, 053817 (2010).